

Article

Room and High-Temperature Wear Behaviour of Al-Based MMCs against an Automotive Brake Pad

Lucia Lattanzi* and Anders Eric Wollmar Jarfors

Department of Materials and Manufacturing, School of Engineering, Jönköping University, Gjuterigatan 5, 55318 Jönköping, Sweden

* Correspondence: lucia.lattanzi@ju.se**How To Cite:** Lattanzi, L.; Jarfors, A.E.W. Room and High-Temperature Wear Behaviour of Al-Based MMCs against an Automotive Brake Pad. *Progress in Composite Materials* 2025, 1(1), 4. <https://doi.org/10.53941/pcm.2025.100004>

Received: 29 November 2024

Revised: 27 December 2024

Accepted: 31 December 2024

Published: 6 January 2025

Abstract: Aluminium metal matrix composites are promising materials for automotive brake discs, and it is critical to assess their wear performance in different braking conditions. This article presents the wear behaviour of aluminium-based composites with different Al-Si matrix alloys added with nickel and copper to retain mechanical strength at high temperatures. The wear tests were conducted at room and high temperatures (250 and 400 °C) to simulate different braking conditions on a pin-on-plate tribometer. The coefficient of friction is in the range of 0.15–0.17 for all materials at room temperature. The specific wear rates of the brake pad and the disc materials indicate that material transfer occurs from the brake pad to the metal counterpart. Microscopy investigations of the wear tracks confirm the material transfer on the composites. It protects the composite surface from wear damage and maintains a stable coefficient of friction. To translate these results into real-world scenarios, the findings of this study suggest that aluminium-based metal matrix composite brake discs have a longer product lifespan compared to the grey cast iron brake discs; the brake pads for the composites would be the components to need replacement due to wear during the product life instead of the brake discs.

Keywords: aluminium; metal matrix composite; wear; friction; tribology; microscopy

1. Introduction

The development of lightweight solutions is becoming increasingly urgent every year to reduce pollution due to transport in terms of fuel consumption, CO₂ emissions [1], and particulate matter (PM) emissions [2,3]. The latter is the focus of the new Euro 7 regulation, which sets for the first time a limit for PM₁₀ (particulate matter below 10 µm in diameter) emission from brake wear [4]. Grey cast iron (GCI) brake rotors contribute to generating non-exhaust PM emissions owing to their poor wear and corrosion resistance, and mechanical braking is seldom used in the electric vehicles that now penetrate the global market. Considering these aspects, efforts have been made to substitute grey cast iron in heavy components, such as brake discs and pistons, with aluminium-based metal matrix composites (MMCs) reinforced with ceramic particles. The interest in Al-MMCs for automotive applications began at the beginning of the century [5–7], with a focus on the wear performance by Llorca [8] and Louis [9], and has increased in recent years. Dolata et al. [10] investigated the possibility of using Al-MMCs reinforced with silicon carbide (SiC) particles in piston-rings-cylinder liner assembly. The authors reported that the Al-MMCs showed significantly better tribological properties than the reference material and could be used for the studied applications. Awe and Thomas [11] presented the potential of Al-based MMC for automotive brake discs, particularly for electric vehicles, thanks to their excellent durability in terms of wear and corrosion resistance.

Several factors influence tribology in MMCs: matrix alloy composition [12,13], reinforcement fraction [14] and size [15], wear conditions like load [16] and sliding speed [6], and temperature [8].



The effect of the matrix alloy composition in Al-based MMCs was investigated by Du et al. [12] and Lattanzi et al. [13] in previous work. Du et al. [12] investigated adding rare-earth elements, lanthanum and cerium, and transition metals, nickel (Ni) and copper (Cu), in the Al-Si matrix alloy to improve its mechanical properties at high temperatures. Different composites reinforced with SiC particles were tested by sliding against brake pad material, and in all cases, an iron-based tribolayer formed during wear. This tribolayer protected the matrix alloy from further damage, but the intermetallic phases limited its development. Lattanzi et al. [13] investigated the effect of adding Ni and zirconium (Zr) to the matrix alloy to increase the composite's maximum operating temperature. The coefficient of friction decreased as wear proceeded, suggesting a protective role of the tribolayer independent of the presence of Ni and Zr. In the presented literature, the Al matrix alloy was added with specific elements to improve its mechanical resistance at high temperatures, but the wear performance was evaluated at room temperature

The effect of temperature on the wear behaviour of Al-based composites was investigated by Martín et al. [8]. The temperature range was 20–200 °C, and there was a transition from mild to severe wear with increasing temperature. The transition occurred between 100 and 150 °C for the unreinforced alloy and between 150 and 200 °C for the composite. The severe wear damage was observed as extensive cracking in the matrix, and the hard phases (intermetallic particles and reinforcing particles) were fragmented. The SiC reinforcement delayed the wear damage transition to higher temperatures.

Despite the renewed interest in Al-based metal matrix composites in recent years and their promising possibility to be employed in automotive components that demand wear resistance, there is a research gap in evaluating the effect of temperature on their wear performance, and the role played by the matrix alloy. This study aims to characterise Al-based metal matrix composites with different compositions of matrix alloys, developed with the specific aim of high-temperature wear. The targeted application of these materials is in the automotive industry, particularly in the automotive brake discs of passenger cars. The currently available solution, SICALight, developed by Automotive Components Floby [11], has a maximum operating temperature of 420 °C. Ni and Cu were added to the matrix alloy to improve its mechanical resistance above the target temperature of 420 °C. The present work is a preliminary study to characterise the wear behaviour of the composites on a pin-on-plate tribometer equipped with a heating unit to perform wear tests at room and high temperatures. The study has the twofold target of evaluating the performance of the equipment and that the materials' performance suits their application in automotive brake discs.

2. Materials and Methods

Automotive Components Floby AB (Floby, Sweden) provided the investigated materials. The composites were produced by squeeze casting, with a targeted SiC content of 20 wt.%. The details of the melt and SiC particle stirring and the squeeze casting procedure are described in previous work [13]. Table 1 lists the chemical compositions of the composites, which were measured by optical emission spectrometry. The Si content in Table 1 provides the total silicon (Si) amount, the sum of the Si in the base alloy, and the Si in the SiCp for each MMC material.

The typical GCI used in brake discs was also investigated for comparison with the composites. The main alloying elements are 3.7 wt.% of carbon (C), 2 wt.% of Si, 0.7 wt.% of manganese (Mn), 0.05 wt.% of phosphorous (P), 0.14 wt.% of sulphur (S), 0.10 wt.% of chromium (Cr), 0.17 wt.% of Cu.

Table 1. Chemical composition (wt.%) of the investigated composites as disc materials.

MMC	Si	Fe	Cu	Mn	Mg	Cr	Ni	Ti	Zr	Al
Mat 000	17.34	0.20	0.01	0.03	0.34	0.02	0.02	0.09	0.00	Bal
Mat 300	20.12	0.22	0.03	0.38	0.64	0.19	3.47	0.13	0.20	Bal
Mat 350	18.50	0.17	0.48	0.11	0.55	0.02	3.44	0.11	0.05	Bal

The microstructure was investigated by optical (DSX 1000, Olympus Europa, Hamburg, Germany) and scanning electron microscopy (SEM) (Mira4, Tescan, Brno, Czech Republic) after standard metallographic preparation. The different phases were identified by energy-dispersive X-ray spectroscopy (EDS) (Apollo, EDAX Ametek, Tilburg, The Netherlands).

The wear test configuration is summarised in Figure 1. Wear tests were performed on a reciprocating pin-on-plate tribometer at room temperature, according to the ASTM G133-05 (2010) standard [17]. The tests at 250 and 400 °C were performed by adding a heating unit below the plate and a thermocouple on the surface of the plate to monitor the temperature. The targeted temperatures were reached in all cases on the surface of the plate and

maintained during the test duration. Insulating material layers minimised heat transfer to the load cell and the rest of the tribometer.

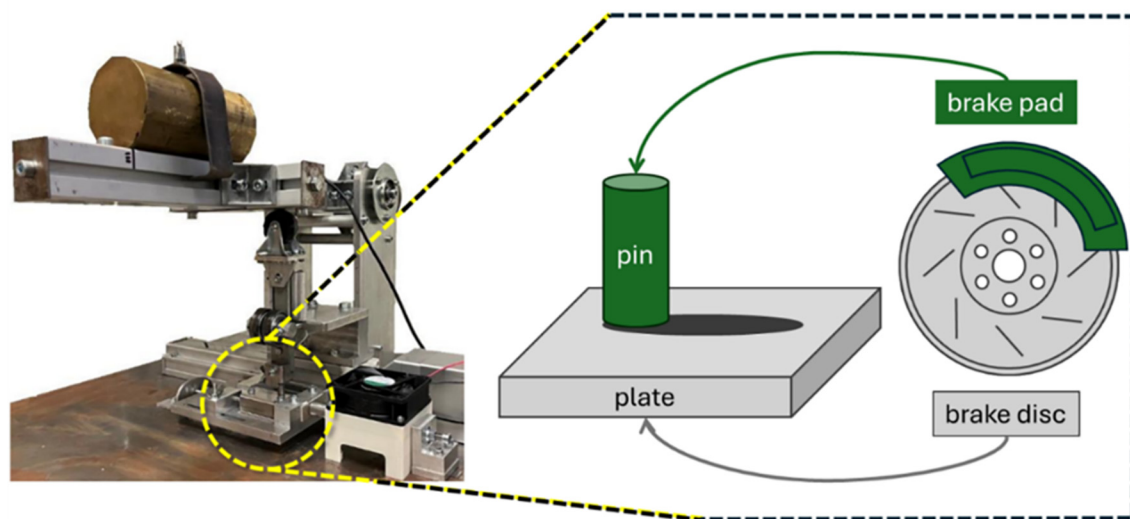


Figure 1. Picture of the pin-on-plate wear rig and schematics of the wear test configuration (adapted from previous work [12]).

The applied load was 112.5 N on pins of 8 mm diameter to have a contact pressure of 2.2 MPa. The average speed was 120 mm/s, the stroke length was 20 mm, and the testing frequency was 1.3 cycles/s. According to the ASTM G133-05 standard, one cycle consists of two stroke lengths, and the total sliding distance (m) is calculated as $0.002 \times \text{time} \times \text{frequency} \times \text{stroke length}$ [17]. The tests lasted one hour, and two samples were tested for each condition. The counter material on the pins was a non-asbestos organic (NAO) brake pad, the zero-copper formulation FER9701, produced and provided by Federal-Mogul Bremsbelag GmbH (Glinde, Germany) for aluminium-based MMC brake discs.

The Archard wear relationship in Equation (1) is used to calculate the specific wear rate. K_α ($\text{mm}^3/\text{N}\cdot\text{m}$): F is the load (N), Δs is the sliding distance (m), Δw is the weight loss (g) and ρ is the density (kg/m^3).

$$K_\alpha = \frac{\Delta w}{\rho F \Delta s} \left[\frac{\text{mm}^3}{\text{N} \times \text{m}} \right] \quad (1)$$

The density values used for the calculations are $2.7 \text{ g}/\text{cm}^3$ for the MMCs and $2.6 \text{ g}/\text{cm}^3$ for the brake pads. The wear surfaces were investigated by an SEM (Mira4, Tescan, Czech Republic) equipped with an EDS probe (Octane, EDAX Ametek, The Netherlands).

3. Results

3.1. Microstructure

The microstructure of the investigated composites observed by optical microscopy is presented in Figure 2. Mat000 (Figure 2a) is the reference composite material and consists of an Al-Si alloy reinforced with SiC particles. The SiC particles appear as dark polygonal features and are common to all the investigated materials. The addition of 3.5 wt.% Ni to the matrix alloy determines the formation of Al_3Ni particles that appear as bright features in the Mat300 microstructure (Figure 2b). Thermo-Calc simulations support the identification of the Al_3Ni phase. Adding Cu in Mat350 (Figure 2c) led to a Cu-enrichment of the Ni-based phase and the primary Al dendrites without precipitation of Cu-based phases. Figure 2d presents the typical microstructure of the GCI used as a comparison material representing the traditional automotive brake discs. The microstructure consists of graphite flakes immersed in the Fe matrix. The hardness of the different phases in the composites was evaluated by Berkovich nanoindentation in previous work by Lattanzi and Awe [18], and it is listed in Table 2 for convenience.

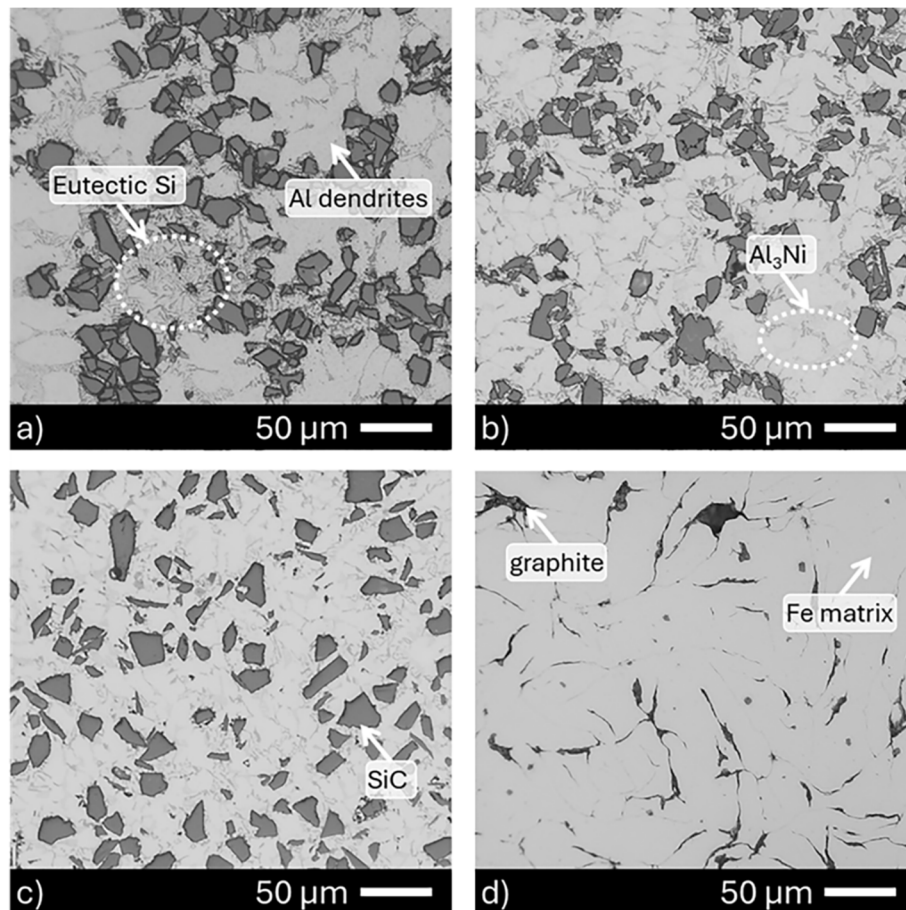


Figure 2. Microstructure of the investigated materials: (a) Mat000; (b) Mat300; (c) Mat350; (d) GCI.

Table 2. The hardness values of the phases in the composites. The values are reproduced from previous work by Lattanzi and Awe [18].

Composite	Phase	Hardness [GPa]
Mat000	Primary Al dendrites	1.00 ± 0.06
Mat000	Eutectic Si particles	2.32 ± 0.22
Mat300	Primary Al dendrites	1.15 ± 0.07
Mat300	Eutectic Si particles	2.73 ± 0.38
Mat300	Al ₃ Ni	3.85 ± 1.35
Mat350	Primary Al dendrites	1.04 ± 0.08
Mat350	Eutectic Si particles	2.45 ± 0.89
Mat350	Al ₃ Ni	3.05 ± 0.48
All	SiC	34.4 ± 3.73

3.2. Wear

Figure 3 presents the coefficient of friction (COF) at different temperatures. Mat000 in Figure 3a presents COF values in the range 0.1–0.2. At room temperature, the COF is stable at 0.15, and the behaviour is similar at 250 °C. The effect of temperature at 400 °C determines an increase of the COF values from 0.1 to 0.2 as the test progresses. Mat300 in Figure 3b presents constant values of COF in the 0.14–0.2, with no evident influence of the temperature on the surface of the plate. Figure 3c shows the COF evolution of Mat350 in the range of 0.08–0.16. The temperature increase determined a decrease in friction to 0.08–0.1 at 250 °C and 0.1–0.12 at 400 °C. Figure 3d shows the COF values of the GCI in the range of 0.06–0.2 at all tested temperatures. The COF values at 250 °C and 400 °C show a transient interval of up to 1000 cycles and then a stable behaviour.

Figure 4 presents the specific wear rate K_{α} (mm³/m³·N) of brake pads (Figure 4a,b) and disc materials (Figure 4c,d). The brake pad tested against GCI presents an increasing wear rate with temperature (Figure 4a), while the wear rates of brake pads peak at 250 °C when tested against the composites (Figure 4b).

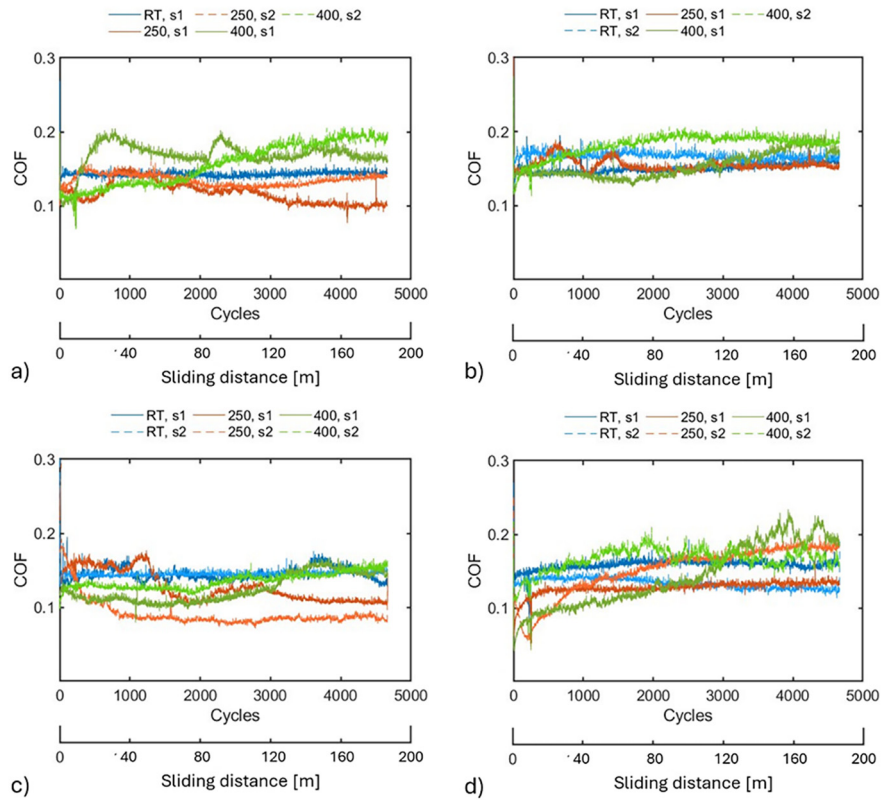


Figure 3. Coefficient of friction (COF) at different temperatures: (a) Mat000, (b) Mat300, (c) Mat350, and (d) GCI. s1 = sample 1; s2 = sample 2.

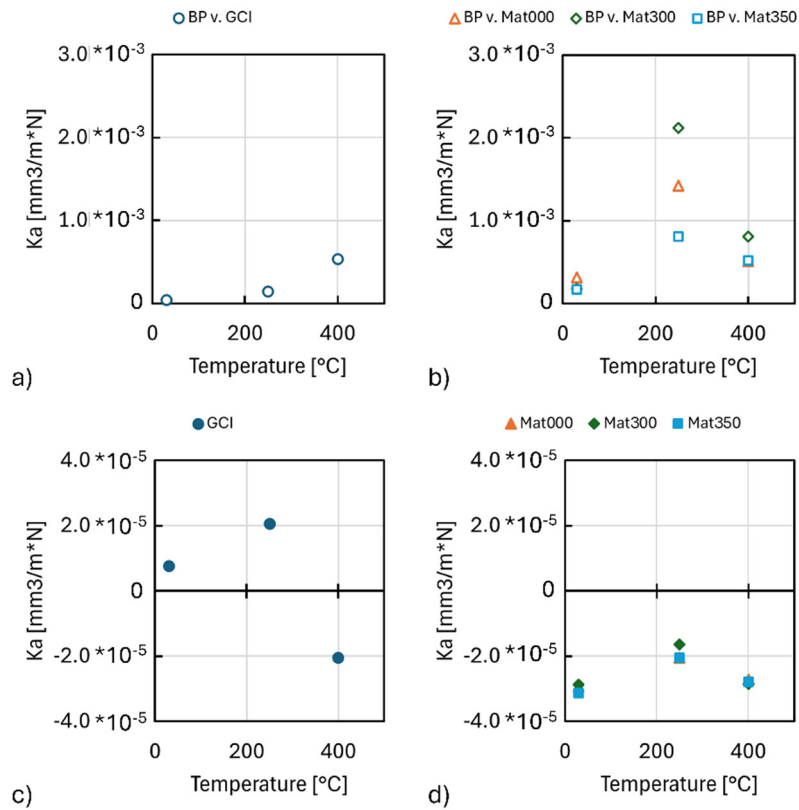


Figure 4. Specific wear rate K_a (mm³/m³·N) of the brake pad (BP): (a) tested against GCI and (b) the composites; specific wear rate K_a (mm³/m³·N) of the disc materials: (c) GCI and (d) composites.

Looking at the wear rate on the metal material side, the GCI presents positive values at room temperature and 250 °C and negative values at 400 °C (Figure 4c). These negative values correspond to material transfer from the brake pad to the metal surface, in line with the peak wear rate for the brake pad at 400 °C in Figure 4a. Figure 4d presents the specific wear rates of the composites, consistently negative values at the tested temperatures. The trend in Figure 4d aligns with the one in Figure 4b and is related to material transfer from the brake pad to the metal surface.

3.3. Wear Tracks

Figure 5 presents the wear track surfaces of the composite materials. The wear track on Mat000 tested at room temperature (Figure 5a) presents portions of aluminium surface worn by abrasion and portions of surface covered by wear residual from the brake pad. Due to its low electrical conductivity, the wear residual appears bright on the secondary electron (SE) image. The surface portions free from the transfer layer often correspond to the presence of SiC particles. The wear track developed at 400 °C (Figure 5b) presents uniform portions of the transfer layer.

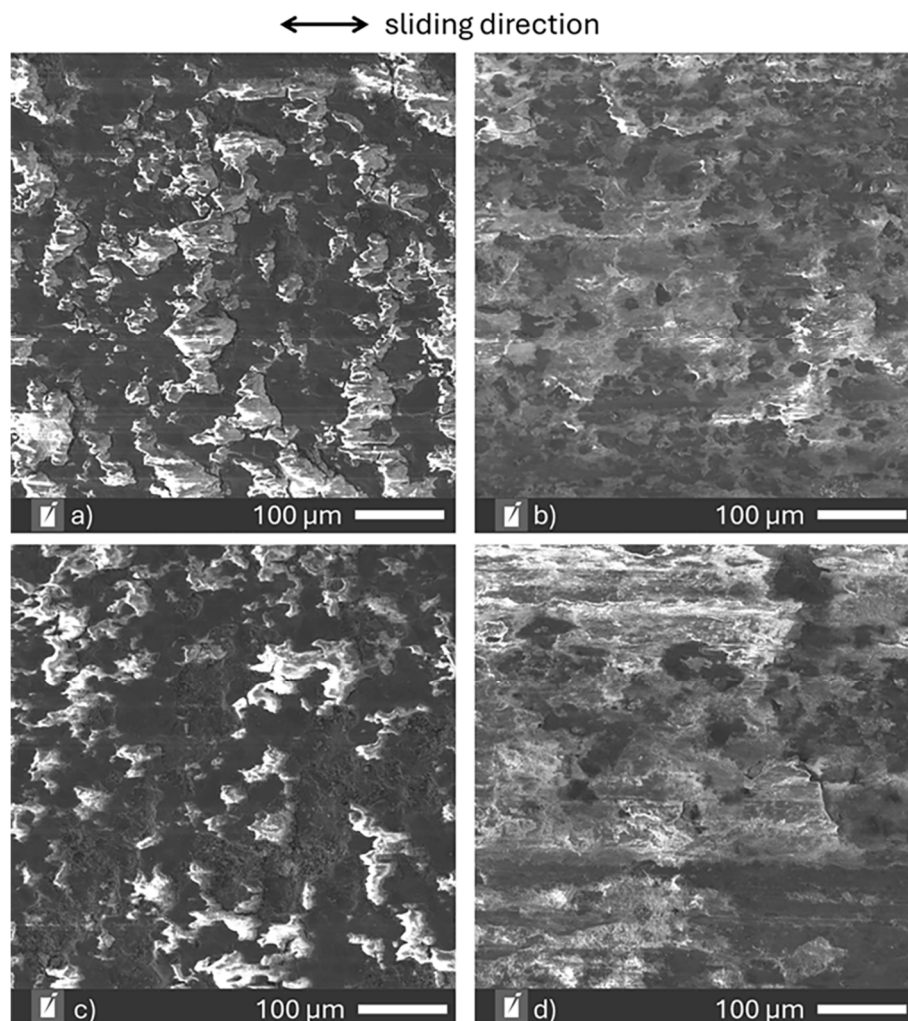


Figure 5. Wear surfaces, SE images: (a) Mat000 tested at room temperature; (b) Mat000 tested at 400 °C; (c) Mat350 tested at room temperature; (d) Mat350 tested at 400 °C.

The wear track on Mat350 tested at room temperature (Figure 5c) is similar in appearance to Mat000 and Mat300, with discontinued portions of the surface covered by wear residual from the brake pad. Figure 5d presents the wear track developed at 400 °C with areas covered by a uniform transfer layer.

EDS point analysis on the wear tracks confirmed the material transfer from the brake pad. Figure 6 shows the EDS points on the wear track of Mat350 tested at 250 °C. The wear surface in Figure 6a shows black polygonal features that are the SiC particles in the composite and the same field of view appears with bright areas that are covered by wear residual.

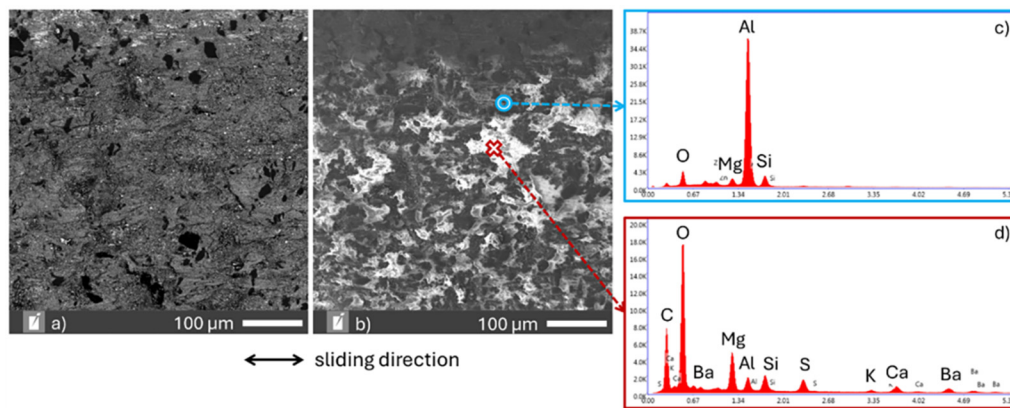


Figure 6. Wear surface of Mat350 at 250 °C: (a) BSE image; (b) SE image with EDS spectra points; (c) EDS spectrum of the point labelled “o”, on the base material; (d) EDS spectrum of the point labelled “x”, on the transfer material.

4. Discussion

The COF values in Figure 3 and the specific wear rates in Figure 4 give insight into the wear mechanisms of the investigated materials, and the wear track investigations in Section 3.3 complete the study.

All materials present a comparable friction behaviour at room temperature, with the COF in the range 0.15–0.17. Similarly, all composites present a negative specific wear rate due to material transfer from the brake pad to the metal counterpart. Conversely, GCI presents a positive wear rate on the metal side, except at 400 °C, and a limited wear rate on the brake pad side.

Mat000 presents a slight decrease in COF at 250 °C (Figure 3a) and a slight increase in wear rate, although in the negative range, which implies weight increase and not weight loss (Figure 4d). The brake pad presented a peak in material loss (Figure 4b) that was not completely transferred to the metal counterpart. The worn brake pad material acted as a lubricant in between the surfaces, determining the observed decrease in friction at 250 °C. Similar observations are valid for Mat350 at 250 °C (Figure 4c). The COF is connected to several aspects of the driving experience, like the braking efficacy and the comfort level, like the noise, vibration, and harshness (NVH) performance. Awe et al. [19] tested the SICAlight discs by brake dynamometer testing setting to compare the NVH performance to the GCI disc. Different braking conditions revealed that the development of the transfer layer on the MMC disc led to stable braking behaviour, limited disc wear, limited thickness variation, and good NVH behaviour.

Figure 7 presents the comparison of the wear tracks of Mat000 at different temperatures. At room temperature (Figure 7a), there is abrasive damage and a discontinuous layer of transfer material from the brake pad; at 250 °C (Figure 7b), the layer of transfer material appears more continuous than the one developed at room temperature and signs of ploughing are visible, likely connected to pulled out SiC particles. These observations align with the COF values of Figure 3a and the specific wear rates of Figure 4b,d.

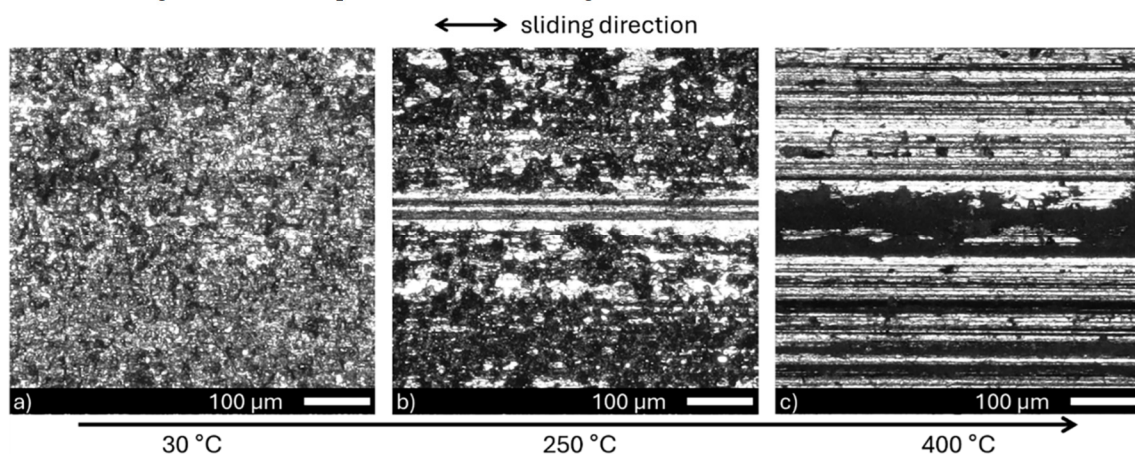


Figure 7. Optical microscope images of the wear tracks on Mat000 tested at: (a) room temperature, 30 °C; (b) 250 °C; (c) 400 °C.

Figure 7c presents the wear track developed at 400 °C with increased signs of ploughing alternated to continuous areas covered by the transfer material from the brake pad. The ploughing signs are related to the increase in COF observed in Figure 3a, while the presence of transfer material clarifies the negative specific wear rate of Figure 4d. The wear tracks of Mat300 and Mat350 present similar features to those observed for Mat000, and the COF at 400 °C is comparable to the value at room temperature, in the range of 0.16–0.2. According to the EDS analysis on the wear tracks in Figure 6 and the specific wear rates in Figure 4, the presence of hard Al₃Ni particles in the matrix alloy did not influence the wear behaviour and the transfer layer development in a significant way. Further analysis of the cross-section of the wear tracks will clarify the role of the microstructural features at high temperatures.

Changes in the wear mechanisms at the interface are reflected as changes in the COF. The transfer layer developed quite early during the wear tests, and its homogeneous presence over the wear tracks (Figure 7a for Mat000) can be connected to the stability of the COF values (Figure 3a for Mat000). On the other hand, the peaks in friction force and COF correspond to damaging wear events like ploughing, of which an example is presented in Figure 7c.

The EDS analysis on the wear tracks clarified the development of transfer material from the brake pad to the composite surface, with the presence of oxygen (O), Mg, Al, Si, sulphur (S), calcium (Ca) and barium (Ba) in the spectra (an example of EDS spectrum in Figure 6d). These elements are present in the brake pad material and not in the base material, as evident by comparing Figure 6c,d. The material transfer aligns with the specific wear rates in Figure 4b,d. Despite the presence of ploughing signs, the development of the transfer layer protects the composite from further wear damage, limiting weight loss and maintaining a constant COF. This mechanism is absent in GCI, which suffers from weight loss (Figure 4c) and an increasing wear rate during the wear tests (Figure 3d).

To translate these results into real-world scenarios, the presented results in terms of wear performance suggest that Al-based MMCs and GCI provide comparable braking performance based on the COF in Figure 3, with Mat300 being the best candidate for a stable COF up to 400 °C. The MMC brake discs would have a longer product lifespan than GCI brake discs. Comparing the material cost listed in the Granta Selector software (Granta Selector 2023 R1, version 23.1.1), it is in the range of 6.2–8.3 €/kg for Duralcan Al-20SiC [20] and in the range of 0.48–0.56 €/kg for cast iron EN GJL 250 [21]. According to Automotive Components Floby, SICAlight (the current MMC available) enables the production of a brake disc that is 50% lighter than its GCI equivalent and up to four times more durable [22]. Table 3 summarises a simple cost evaluation to compare GCI and MMC brake discs.

Table 3. A simple material cost evaluation of GCI and MMC brake discs.

Material	GCI EN GJL 250	Duralcan Al-20SiC
Disc weight (kg)	7	3.5
Material cost (€/kg) *	0.48–0.56	6.2–8.3
Disc material cost (€)	3.36–3.92	21.7–29.05
Disc lifespan (years) **	3	12
Compensated disc material cost (€/year)	1.12–1.3	1.8–2.4

* Data from the Granta Selector database [20,21]. ** Data from the SICAlight website [22].

The MMC material cost is one order of magnitude higher than the GCI material cost, and the brake disc's weight reduction is insufficient to make the disc material cost comparable. When including the lifespan into the calculations, the MMC disc becomes competitive with the GCI ones when looking at the compensated disc material cost.

This simple cost evaluation does not include the costs related to disc production, as the aim is to evaluate the potential benefits of the material itself. Similarly, for a complete life cycle cost analysis, the cost of the brake pads should be included. According to the presented results, the brake pad material should be further developed to mitigate brake pad wear, which demands frequent brake pad replacements.

5. Conclusions

Aluminium metal matrix composites are promising materials for automotive brake discs, and this article assesses their wear performance at different temperatures to simulate the demands of different braking conditions. This article investigates the wear behaviour of aluminium-based composites with different Al-Si matrix alloys added with nickel (Ni) and copper (Cu) to retain mechanical strength at high temperatures. The wear tests were conducted at room and high temperatures, 250 and 400 °C on a pin-on-plate tribometer. Using a heating unit under the plate proved successful in maintaining a constant temperature on the surface during the wear tests. The main conclusions are the following:

- The coefficient of friction is in the range of 0.15–0.17 at room temperature, making the materials comparable. As the temperature increases to 250 °C, the interaction of the composites with the brake pad determines a layer of worn material from the brake pad that decreases the friction at the interface. At 400 °C, ploughing is active and counterbalances the effect of the transfer layer, resulting in an almost stable COF.
- The specific wear rate values indicate wear loss at the expense of the brake pad and positive weight changes for the composite materials. On the other hand, GCI suffers from wear losses and the brake pad presents limited wear loss. The material transfer on the composites protects the surface from wear damage and maintains a stable COF.
- The SEM investigations of the wear tracks confirm the material transfer from the brake pad to the composite material.

To translate these results into real-world scenarios, the findings of this study suggest that aluminium-based metal matrix composite brake discs have a longer product lifespan than GCI brake discs. The brake pad material should be developed to mitigate brake pad wear, which demands frequent brake pad replacements.

From the tribology point of view, the comparable COF values up to 400 °C are promising results to confirm that the aluminium-based composites are suitable candidates to replace GCI in automotive brake discs. Future work will include the assessment of PM emissions to verify the suitability of composite materials for the Euro7 regulation. Given the high temperatures involved, the material characterisation will be integrated by thermogravimetric analysis (TGA) of the aluminium-based composites to assess their oxidation behaviour and correlate it with the development of the transfer layer.

Author Contributions

Conceptualization, L.L. and A.E.W.J.; methodology, L.L.; validation, L.L. and A.E.W.J.; formal analysis, L.L.; investigation, L.L.; resources, A.E.W.J.; data curation, L.L.; writing—original draft preparation, L.L.; writing—review and editing, A.E.W.J.; visualisation, L.L.; project administration, L.L.; funding acquisition, L.L. and A.E.W.J. All authors have read and agreed to the published version of the manuscript.

Funding

This research was funded by the Stiftelsen för kunskaps- och kompetensutveckling (KK-Stiftelsen), Sweden, through the project “Properties and formability of Al-SiCp MMCs” (ProForAl) [Prospekt, diariennr. 20201702].

Data Availability Statement

Data will be made available on request.

Acknowledgments

The authors gratefully acknowledge the ProForAl project partners: Samuel Awe at Automotive Components Floby AB, Per Jansson at Comptech i Skillingaryd AB, Richard Westergård at Gränges Finspång AB and Carl Rudenstam at Husqvarna Group AB. Maxime Beaufort is gratefully acknowledged for performing part of the experiments during his internship at Jönköping University. Ansys is gratefully acknowledged for providing Granta Selector software through the Research Partnership with Tekniska Högskolan i Jönköping.

Conflicts of Interest

The authors declare no conflict of interest.

References

1. Serrenho, A.C.; Norman, J.B.; Allwood, J.M. The impact of reducing car weight on global emissions: The future fleet in Great Britain. *Philosophical Transactions of the Royal Society A: Mathematical. Phys. Eng. Sci.* **2017**, *375*, 20160364. <https://doi.org/10.1098/rsta.2016.0364>.
2. Grigoratos, T.; Martini, G. Brake wear particle emissions: A review. *Environ. Sci. Pollut. Res.* **2015**, *22*, 2491–2504. <https://doi.org/10.1007/s11356-014-3696-8>.
3. Perricone, G.; Matějka, V.; Alemani, M.; et al. A concept for reducing PM10 emissions for car brakes by 50%. *Wear* **2018**, *396–397*, 135–145. <https://doi.org/10.1016/j.wear.2017.06.018>.

4. European Vehicle Emissions Standards—Euro 7 for Cars, Vans, Lorries and Buses n.d. Available online: https://ec.europa.eu/info/law/better-regulation/have-your-say/initiatives/12313-European-vehicle-emissions-standards-Euro-7-for-cars-vans-lorries-and-buses_en (accessed on 23 June 2022).
5. Vencl, A.; Rac, A.; Bobić, I. Tribological behaviour of Al-based MMCs and their application in automotive industry. *Tribol. Ind.* **2004**, *26*, 31–38.
6. Ravikiran, A.; Surappa, M.K. Effect of sliding speed on wear behaviour of A356 Al-30 wt.% SiCp MMC. *Wear* **1997**, *206*, 33–38. [https://doi.org/10.1016/S0043-1648\(96\)07341-3](https://doi.org/10.1016/S0043-1648(96)07341-3).
7. Narciso, J.; García-Cordovilla, C.; Louis, E. Reactivity of thermally oxidized and unoxidized SiC particulates with aluminium-silicon alloys. *Mater. Sci. Eng. B* **1992**, *15*, 148–155. [https://doi.org/10.1016/0921-5107\(92\)90047-D](https://doi.org/10.1016/0921-5107(92)90047-D).
8. Martín, A.; Martínez, M.A.; Llorca, J. Wear of SiC-reinforced Al-matrix composites in the temperature range 20–200 °C. *Wear* **1996**, *193*, 169–179. [https://doi.org/10.1016/0043-1648\(95\)06704-3](https://doi.org/10.1016/0043-1648(95)06704-3).
9. García-Cordovilla, C.; Narciso, J.; Louis, E. Abrasive wear resistance of aluminium alloy/ceramic particulate composites. *Wear* **1996**, *192*, 170–177. [https://doi.org/10.1016/0043-1648\(95\)06801-5](https://doi.org/10.1016/0043-1648(95)06801-5).
10. Dolata, A.J.; Wiecek, J.; Dyzia, M.; et al. Assessment of the Tribological Properties of Aluminum Matrix Composites Intended for Cooperation with Piston Rings in Combustion Engines. *Materials* **2022**, *15*, 3806. <https://doi.org/10.3390/ma15113806>.
11. Awe, S.; Thomas, A. The Prospects of Lightweight SiC/Al Discs in the Emerging Disc Brake Requirements. *E Transp.* **2021**, *13*, 14. <https://doi.org/10.46720/5965299eb2021-mds-012>.
12. Du, A.; Lattanzi, L.; Jarfors, A.E.W.; et al. Role of matrix alloy, reinforcement size and fraction in the sliding wear behaviour of Al-SiCp MMCs against brake pad material. *Wear* **2023**, *530–531*, 204969. <https://doi.org/10.1016/j.wear.2023.204969>.
13. Lattanzi, L.; Etienne, A.; Li, Z.; et al. The effect of Ni and Zr additions on hardness, elastic modulus and wear performance of Al-SiCp composite. *Tribol. Int.* **2022**, *169*, 107478. <https://doi.org/10.1016/j.triboint.2022.107478>.
14. Agnihotri, R. Mechanical Properties of Al-SiC Metal Matrix Composites Fabricated by Stir Casting Route. *Res. Med. Eng. Sci.* **2017**, *2*, 1–6. <https://doi.org/10.31031/rmes.2017.02.000549>.
15. Lee, T.; Lee, J.; Lee, D.; et al. Effects of particle size and surface modification of SiC on the wear behavior of high volume fraction Al/SiCp composites. *J. Alloys Compd.* **2020**, *831*, 154647. <https://doi.org/10.1016/J.JALLCOM.2020.154647>.
16. Gultekin, D.; Uysal, M.; Aslan, S.; et al. The effects of applied load on the coefficient of friction in Cu-MMC brake pad/Al-SiCp MMC brake disc system. *Wear* **2010**, *270*, 73–82. <https://doi.org/10.1016/j.wear.2010.09.001>.
17. G133; Standard Test Method for Linearly Reciprocating Ball-on-Flat Sliding Wear. ASTM International: West Conshohocken, PA, USA, 2010. <https://doi.org/10.1520/G0133-05R10.2>.
18. Lattanzi, L.; Awe, S.A. Thermophysical properties of Al-based metal matrix composites suitable for automotive brake discs. *J. Alloys Metall. Syst.* **2024**, *5*, 100059. <https://doi.org/10.1016/J.JALMES.2024.100059>.
19. Awe, S.; Eilers, E.; Gulden, F. Sustainable Aluminium Brake Discs and Pads for Electrified Vehicles. Eurobrake 2023; FISITA: Barcelona, Spain, 2023. <https://doi.org/10.46720/EB2023-TST-020>.
20. *Granta Selector A 2023 R1 (Duralcan Al-20SiC (p) cast (F3K20S))*; Version 23.1; Ansys: Canonsburg, PA, USA
21. *Granta Selector A. 2023 R1 (EN GJL 250 2023)*; version 23.1; Ansys: Ansys: Canonsburg, PA, USA
22. SiCAlight—AC Floby n.d. Available online: <https://www.sicalight.com/> (accessed on 1 March 2024).